

Victor V. Kharitonov^{1*}

¹Arctic and Antarctic Research Institute, St. Petersburg, Russia

* **Corresponding author:** sogra.kharitonov@mail.ru

ICE RIDGES IN LANDFAST ICE OF SHOKAL'SKOGO STRAIT

ABSTRACT. Three first-year ice ridges have been examined with respect to geometry and morphology in landfast ice of Shokal'skogo Strait (Severnaya Zemlya Archipelago) in May 2018. Two of the studied ice ridges were located on the edge of the ridged field and were part of it, because their keels extended for a long distance deep into this field. Ice ridges characteristics are discussed in the paper. These studies were conducted using hot water thermal drilling with computer recording of the penetration rate. Boreholes were drilled along the cross-section of the ridge crest at 0.25 m intervals. Cross-sectional profiles of ice ridges are illustrated. The maximal sail height varied from 2.9 up to 3.2 m, the maximal keel depth varied from 8.5 up to 9.6 m. The average keel depth to sail height ratio varied from 2.8 to 3.3, and the thickness of the consolidated layer was 2.5-3.5 m. The porosity of the non-consolidated part of the keel was about 23-27%. The distributions of porosity versus depth for all ice ridges are presented.

KEY WORDS: ice ridge, water thermal drilling, cross-sectional profile, consolidated layer, porosity

CITATION: Victor V. Kharitonov (2019) Ice ridges in landfast ice of Shokal'skogo Strait. *Geography, Environment, Sustainability*, Vol.12, No 3, p. 16-26
DOI-10.24057/2071-9388-2019-43

INTRODUCTION

Studies of morphometric characteristics of ridged features as the thickest areas of ice cover, unlike similar studies of the morphometry of non-deformed ice, do not have a rich history, and the amount of currently available observational data cannot be considered sufficient (Sudom & Timco 2013). Active studies of ice ridges on the shelf of freezing seas of Russia are conducted, since their morphometric characteristics, primarily the thickness of the ice ridge consolidated layer (CL), should be taken into account at the designing stage in the assessment of possible loads on the structures. And the information about these characteristics is still being supplemented. However, there are very few studies on the morphometry of deformed and ridged ice in the Laptev

and East-Siberian Seas, and for Shokal'skogo Strait, in particular, such information is not available. Under the conditions of changing climate, reduction of ice area in the Arctic Ocean and decreasing ice thickness, any information on the internal structure of modern ice ridges is of undoubted value.

SITE AND EXPERIMENTAL METHODS

This paper presents the information on morphometric characteristics and the internal structure of three ice ridges in landfast ice of Shokal'skogo Strait in the Severnaya Zemlya Archipelago obtained between April, 13 and May, 31, 2018 (Fig. 1). The working team was accommodated at the "Ice base "Cape Baranov" station belonging to the Arctic and Antarctic Research Institute (AARI).

Investigation of the structure of ice ridges was carried out by means of hot water thermal drilling unit of AARI comprising heater, thermal drill and equipment for penetration rate recording on a logger. The power was supplied by a 4 kW generator. A general view of hot water ice drilling unit is presented in Fig. 2. An example of recording the penetration rate of ice ridge drilling and reconstruction of its structure is presented in Fig. 3. Drilling was carried out along the profile up to reaching level ice. A few boreholes were drilled on the level ice.

The ice ridge geometry and internal structure are retrieved by processing

the thermodrilling records (Morev et al. 2000; Mironov et al. 2003; Kharitonov & Morev 2011). The drilling rate depends on the power supply, ice porosity and ice temperature. The location of voids, hard and porous ice along the drilling hole is identified by the thermodrill penetration rate. The obligatory condition for this identification to be valid is drilling at constant thermal capacity or recording the changes of capacity during drilling. Within the segments of porous ice and, especially, the voids filled by snow, shuga or air, the penetration rate of thermodrill sharply increases. In addition, the distance from snow (ice) surface to the sea level



Fig. 1. Map of the area of work. The 'plus' sign indicates the position of the three ridges



Fig. 2. General view of hot water ice drilling unit UVBL-2. The picture shows the operation of two drilling stations. In 2018, drilling of ice ridges was conducted using one station

is measured. The thermodrilling data processing gives such characteristics as the above-water and under-water parts of the ice cover, the boundaries of the ice ridge CL, the boundaries of the voids and the boundaries of ice layers of various porosities.

RESULTS AND DISCUSSION

During the period from 13.04.18 to 31.05.18, three ice ridges were examined in detail.

Their main morphometric characteristics are demonstrated in Table 1. The three investigated ridges are labeled in Fig. 4.

On each ice ridge the thermal drilling of boreholes along the profile perpendicularly cutting the ice ridge crest was carried out. To the right of ice ridge 1 there was a first-year ice floe with a thickness of 1.2 m. On the photo, the drilling profile of ice ridge 1 was made along the line connecting the right edge of the snow inflation to the right

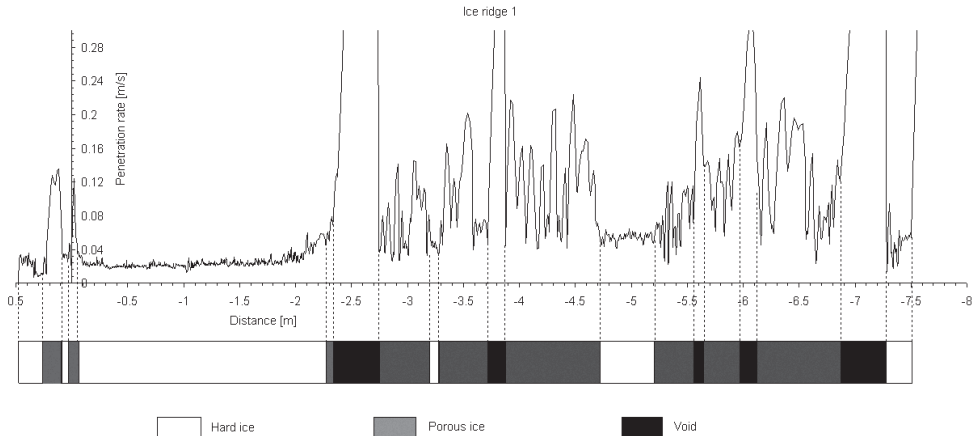


Fig. 3. Example of thermal drilling record. A strip is drawn under the diagram schematically showing ice ridge structure at the drilling point. White colour shows areas along the borehole corresponding to hard ice; grey colour, areas corresponding to porous ice or drill transition from ice into void; and black colour, voids. Dotted lines show boundaries of these areas



Fig. 4. Photo of investigated ice ridges (by Andrey Paramzin). The labels correspond to the ridge' ID. Lines show location of the profiles

Table 1. Basic characteristics of investigated ice ridges (by records of hot water thermal drilling)

	Ice ridge		
	1	2	3
Number of boreholes	267	81	93
Average/maximum ice thickness [m]	7.39/11.22	8.07/10.60	7.64/12.07
Average/maximum sail height [m]	1.82*/3.18	1.61/2.88	1.27/2.87
Average/maximum keel depth [m]	6.62/9.04	7.43/8.49	6.56/9.59
Average position of the upper boundary of CL [m]	-0.11	-0.19	-0.54
Average position of the lower boundary of CL [m]	-2.62	-3.70	-3.48
Minimum/average/maximum CL thickness [m]	1.3/2.5/4.0	2.0/3.5/4.2	1.7/2.9/4.3
Minimum/average/maximum level ice thickness nearby ice ridge [m]	1.20**	1.97***/3.03*** /2.40	1.70***/2.58*** /2.94
Number of measurements of the ice block thickness	54	10	25
Average thickness of ice blocks in the ice ridge sail [m]	0.29* & 0.19****	0.27	0.20* & 0.35****
Sail slope angle [degree]	38.5-52.6*	30.7-84.4	22.7-44.3*
Keel slope angle [degree]	25.0	76.6	38.6-63.6
Average ice ridge porosity	0.17	0.17	0.13
Average porosity of the unconsolidated part of the keel	0.27	0.25	0.23
Ratio of the maximum keel to maximum sail	2.8	3.0	3.3
Average ratio of the CL thickness to total ice thickness	0.34	0.43	0.38
Ratio of the average CL thickness to average level ice thickness	2.09	-	-
Average/maximum snow thickness on the ice ridge [m]	0.41/1.56	0.78/1.60	0.48/1.54

* Main ice ridge crest.

** Four boreholes were drilled on the level ice 1.20 m thick.

*** Due to a large size of the rafted ice field, the location of level ice was not reached. The measurements correspond to rafted ice thickness.

**** Second ice ridge crest.

of the ridge and the place where the two ice explorers are. The distance between the leftmost borehole on the profile and the ice ridge crest was 50 m. Drilling profile of ice ridge 2 was approximately parallel to the drilling profile of ice ridge 1. Ridged ice was to the right of the crest of ice ridge 2 and to the left – rafted ice with a thickness of 2-3 m (2.4 m on average). Drilling profile of ice ridge 3 was perpendicular to the drilling profile of ice ridge 2.

Boreholes were spaced at 0.25 m. At the edges of the profiles, where ice ridge consolidation reached 100 %, drilling was performed at a spacing of 0.5-1 m. At each point, snow cover thickness and ice surface elevation above sea level were measured. Besides, 3D-model of upper surface of ice was obtained by processing

of materials of aerial photography survey. Visual examination of the lower surface of ice ridge 1 was also performed using a remotely operated underwater vehicle (ROV) “Gnom” and a sonar (Borodkin et al. 2018). As a result of sonar data processing, it turned out that the crest of the keel of ice ridge 1 is dislocated aside and extends on significant distance perpendicularly to the crest of the sail (Fig. 5). It is a coincidence that the drilling profile runs just along the crest of the keel. Unfortunately, apparently due to an error in the sonar settings the scales are misrepresented to a large degree.

Figs. 6-8 show the profiles of the investigated ice ridges.

Average thickness of ice blocks in the main sail crest of ice ridge 1 was 0.29 m (located

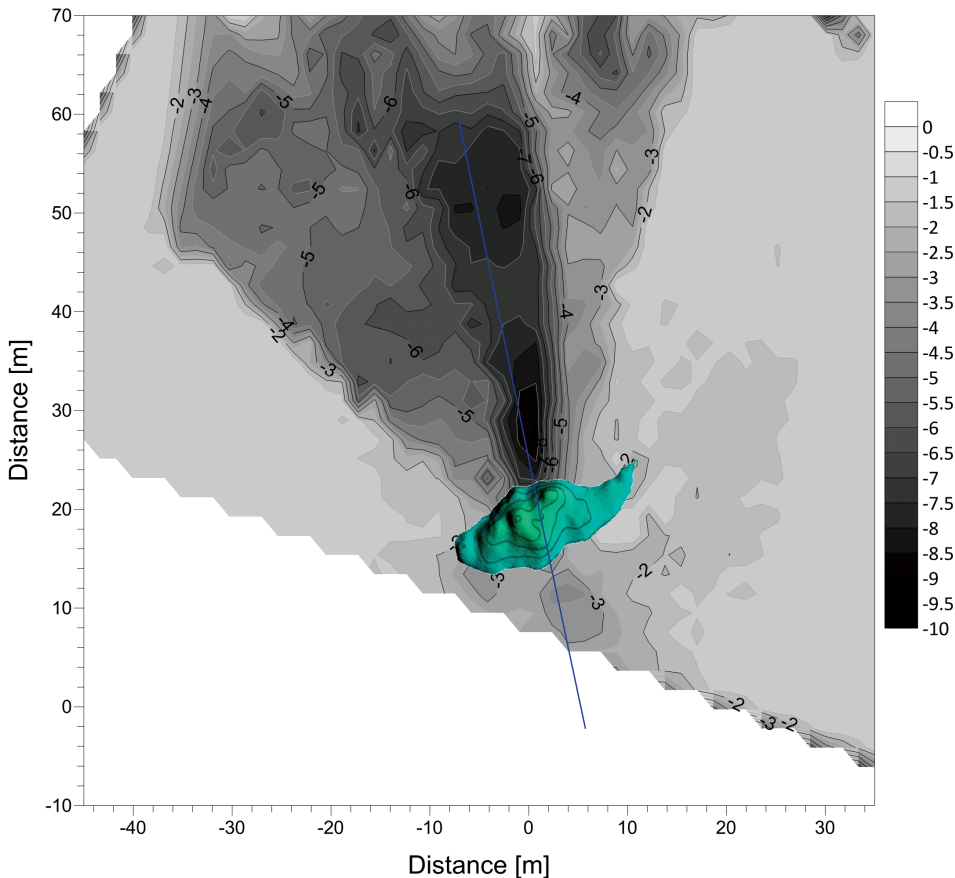


Fig. 5.Relief of the lower ice ridge 1 surface. The crest of the ice ridge sail is shown on the diagram in green and cut off along the excess contour of 2 m. The secant line (straight line in the diagram) run perpendicular to the sail crest of ice ridge 1. Keel draft along the drilling profile is shown below

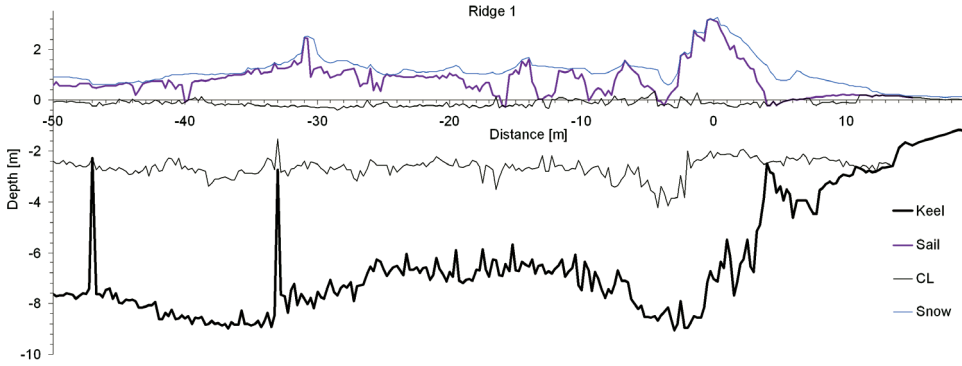


Fig. 6. Resulting cross-sectional profile of thermodrilling of ice ridge 1

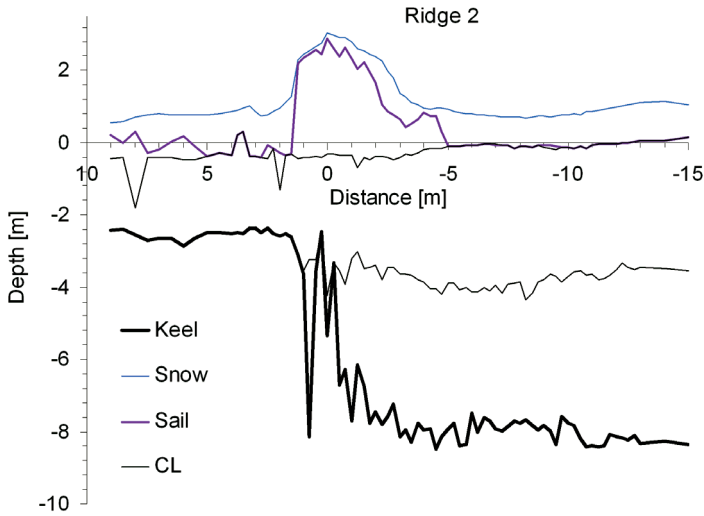


Fig. 7. Resulting cross-sectional profile of thermodrilling of ice ridge 2

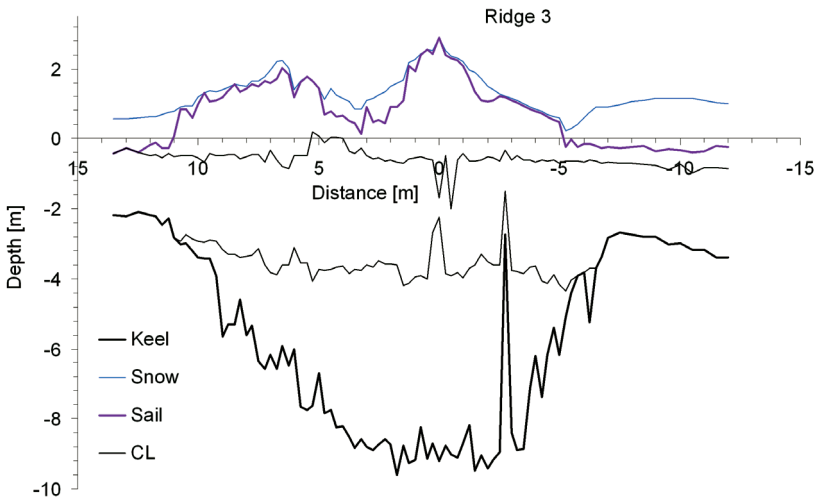


Fig. 8. Resulting cross-sectional profile of thermodrilling of ice ridge 3

at the distance 0 m in Fig. 6), and in the second sail crest (located at the distance of -31 m in Fig. 6) – 0.19 m. That means that the main crest of ice ridge 1 is the result of secondary ridging. One of the signs of the secondary ice ridges is a formation of two or several above-water parts of them, located most often at an angle to each other markedly differing in the thickness of the ice fragments (Tyshko and Kharitonov 2011). The crest with a higher sail in the ice ridge 1 was formed later, at the final stage of ridging. Ice ridge 2 has the extremely large angles of sail and keel slope (84° and 77°) from the side of rafted ice. Apparently, the keel left slope edge has a fairly loose structure as at a distance of $-0.25 \dots 0.5$ m. There was almost no ice blocks detected while drilling below the CL. Ice ridge 2 was covered with a thick snow layer. Judging by the block thickness in its sail (0.27 m), the ridge 2 was formed approximately during the same period of time as the main crest of ice ridge 1. Two crests of the sail of ice ridge 3 are also formed from ice of various thickness: the average blocks thickness of the highest pile of ice ridge sail (see Fig. 8) was 0.20 m (a mode of distribution was 0.11 m), of the more flat pile – 0.35 m (a mode of distribution was 0.32 m). Hence, the ice ridge 3 was formed in two stages as the two other ridges. There is also a noticeable submerging of the ice ridge 3. In case of ice ridges 1 and 2 it was not succeed to extend the drilling profile in both directions up to reaching level ice. There was an impression that we are on the edge of ridged field of great length. Decisions were made to proceed to the next objects.

Recently, the focus of scientists studying ridged features shifted towards the little-known, but rather interesting problem of CL thickness distribution within a ridged feature. Information for resolving this problem is also provided by our study. Average thickness of the CL of ice ridge 1 is 2.5 m; the maximum one is 4.0 m; the minimum one is 1.3 m. The CL is well developed and non-uniform in its thickness. Unlike the first ice ridge, on ice ridge 2, the thickness of the CL ranges within $2.0 \dots 4.2$ m; the CL is thick in the right part

of the profile, slightly thinner under the sail, which can be associated with screening by the sail and a barrier for penetration of cold to the ice ridge keel. The CL of ice ridge 3 is slightly thinner ($1.7 \dots 4.3$ m) than that of ice ridges 1 and 2. However, it is immersed significantly; the average location of the upper CL boundary is at the depth of -0.5 m, at some points up to -1 m. The CL thickness of ice ridges of the Shokal'skogo Strait is noticeably higher than that, for example, near the Spitsbergen archipelago and the Fram Strait. Their CL thickness is $1.0 \dots 2.8$ m on average (Bonnemaire et al. 2003; Høyland 2002, 2007; Bonath et al. 2018). In the paper (Strub-Klein and Sudom 2012), the average CL thickness of 117 ice ridges equals 1.6 m. Mironov and Porubaev (2005, 2012) give the average CL thickness in the range of $1 \dots 3.6$ m. Undisturbed level ice is located near the ice ridge 1 and the ratio of the average CL thickness to level ice thickness is 2.1 . For the ice ridges investigated by Bonath et al. (2018), this ratio is $1.4 \dots 3$, predominantly $2 \dots 3$. It is suggested in ISO19906 (2010) that the CL thickness can be assumed to be two times the level ice thickness. Nevertheless, from the author's experience of studying 229 ice ridges, this ratio is 1.6 on average.

Thickness of the CL does not definitely correlate with the porosity of the unconsolidated portion of the keel and with the snow cover thickness; however, there is a significant reverse correlation with snow/ice elevation above sea level (correlation coefficients -0.32 , -0.72 and -0.31 for the investigated ice ridges). Therefore, it can be stated that the CL of the studied ice ridges was determined, to a larger extent, by the access of cold to the unconsolidated keel. In most cases, in the portion of the keel covered by the sail or a thick snow cover the CL is slightly thinner. Høyland and Løset observed a similar pattern (1999).

In the central part of the ice ridge 3, the CL has a few voids. Judging by the fact that the CL thickness is rather large in the neighboring boreholes, there should not be sharp differences in the location of CL boundaries between neighboring points. Despite of this, in Fig. 8, the small

CL thickness in this zone is designated approximately. This is, most likely, due to the screening by the sail and preventing cold penetration to the ice ridge keel.

Taking the selected criterion for determination of voids (Mironov et al. 2003) into account, the penetration rate record at every point of drilling can be realised as the staircase curve, where zero corresponds to ice, and one corresponds to voids. All depths are considered in sequence from the maximum ice ridge sail height to the maximum ice ridge keel depth. For all boreholes where the depth under consideration is not beyond the freeboard or the keel lower boundary, values of the staircase curves (0 or 1) are averaged. As a result, the depth-wise distribution of porosity is obtained.

Fig. 9 shows such distribution for the studied ice ridges. In Fig.9c, the porosity below -9 m is cut off at 0.6. The cause of this very high porosity values is the low number of observation for this depth. As may be noticed from Fig. 9 and, especially from Figs. 9b and 9c, the freeboard porosity increases within the layer separating the sail from the CL. It is located at the depth of $-0.13...0.18$ m (Fig. 9b) and of $0...0.8$ m

(Fig. 9c). But it is rather a virtual layer in the average ice ridge. As these are averaged curves, it means that there are the voids above the CL in 15-40 % of boreholes. The CL is noted for an abrupt decrease in porosity in the area of water level. The longer the ice ridge was subjected to cold, the greater its CL thickness is and the smaller the variation in the position of its lower boundary is. The porosity curve in the area of the CL lower boundary becomes flatter. The averaged keel porosity below the CL increases with depth. It was noted in (Grishchenko 1988) that in fresh (i. e. at the stage before the CL formation) Arctic ice ridges, the porosity at the sea level was by 0.1-0.2 lower than in the ridge top and keel parts. The author connected this peculiarity of porosity distribution by vertical with the action of the gravity and surfacing forces, contributing to concentration and subsequent compacting of small ice fragments in the sea level area. Surkov (2001(a, b)) showed that the keel porosity in ice ridges of the Sea of Okhotsk and the Baltic Sea below the CL increases with depth from 0.27 to 0.4-0.5 (in the lower keel part) by the linear law. The linear dependence of porosity is also noted in (Pavlov et al. 2016).

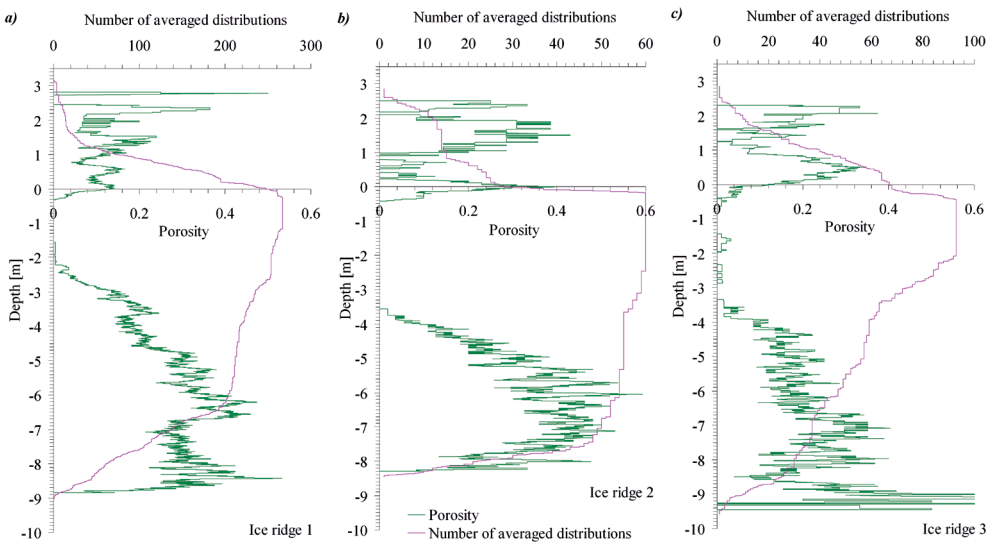


Fig. 9. Depth-wise distribution of the porosity of ice ridges investigated in the Shokal'skogo Strait (Severnaya Zemlya Archipelago) in 2018 (according to the hot water thermal drilling data)

The porosity curve increase of ice ridge 1 with depth has discontinuity at the depth of 6.7 m. As core drilling at a distance of 49 m and subsequent study of ice salinity and texture and also the analysis of penetration rate records showed that there was a large block of two-year ice at a distance of –47...–50 m (Fig.6) at a depth below 6.7 m. The number of the distributions used for averaging is not so considerable at a depth below 6.7 m; therefore, the presence of the large ice block leads to a decrease in the average porosity at that depth.

From literary sources it is known that averaged porosity of the unconsolidated portion of the keel can vary from 0.2 (Strub-Klein and Sudom 2012; Ervik et al. 2018) to 0.3 (Beketsky and Truskov 1995; Høyland 2007), reaching in some cases up to 0.5 (Bonath et al. 2018). As can be seen from the graphs in Figs. 9b and 9c, the porosity in the unconsolidated portion of the keel of ice ridge 2 and 3 is depth-wise distributed differently. However, averaged porosities of the unconsolidated portion of the keel of ice ridge 2 and 3 are practically equal (see Table 1). That is, ice in the keels redistributed. Porosity in the ice ridge 2 quickly reaches high values with depth. Porosity below the CL in the ice ridge 3 varies only slightly, but in the lower part of the keel its values increase.

CONCLUSIONS

The accomplished studies enabled to receive new data on the ice cover of the Shokal'skogo Strait. The following conclusions can be drawn:

– ratios “maximum keel / maximum sail” of the investigated ice ridges were equal to

2.8, 3.0 and 3.3;

– CL thickness of the studied ice ridges varied in the range of 1.3...4.0 m; average values of the CL thickness were 2.5...3.5 m; the formation of CL was owing, to a lesser extent, to the packing density of broken ice in the keel and, to a greater extent, to the access of cold to the unconsolidated keel;

– ratio “average CL thickness / average thickness of level ice”, retrieved for one investigated ice ridge, was equal to 2.1;

– consolidation degree of the investigated ice ridges was about 34-43 %;

– unusual structure of the ice ridge is found, in which the crest of the ice ridge keel is dislocated aside and extends on significant distance perpendicularly to the crest of the sail;

– average porosity of the unconsolidated part of the keel increases with the keel depth.

ACKNOWLEDGEMENTS

Field research was conducted within the seasonal expedition “Sever-2018” organised by the High-Latitudinal Arctic Expeditions Department, the Arctic and Antarctic Research Institute Roshydromet's. I want to thank my colleagues of AARI Gennady Deshevykh and Andrey Shirshov for the assistance in thermodrilling of ice ridges. I express my gratitude to Andrey Paramzin for kindly providing aerial photographs of ice ridges and special thanks ■ Stepan Khotchenkov for the sonar data.

REFERENCES

- Beketsky S.P. & Truskov P.A. (1995). Internal Structure of Ice pressure ridges in the sea of Okhotsk. Proc. of the 13th Int. Conference on Port and Ocean Engineering under Arctic Conditions. August 15-18, 1995. Murmansk, Russia, V. 1, pp. 109-111.
- Bonath V., Petrich C., Sand B., Fransson L., Cwirzen A. (2018). Morphology, internal structure and formation of ice ridges in the sea around Svalbard. *Cold Regions Science and Technology* V. 155, pp. 263-279.
- Bonnemaire B., Høyland K.V., Liferov P. & Moslet P.O. (2003). An ice ridge in the Barents Sea, part I: morphology and physical parameters in-situ. Proc. of the 17th Int. Conf. on Port and Ocean Engineering under Arctic Conditions. June 16-19 2003, Trondheim, Norway.
- Borodkin V.A., Paramzin A.S., Khotchenkov S.V. (2018). Joint application of a multirotor unmanned aerial vehicle and a scanning sonar to create a three-dimensional digital model of the ice feature relief. *Rossiiskie poliarnye issledovaniia. Russian polar research*. 2018, 4: 31-35 [In Russian]. http://www.aari.ru/misc/publicat/sources/34/RPR-34el_l_30-34.pdf
- Ervik Å., Høyland K.V., Shestov A., Nord T.S. (2018). On the decay of first-year ice ridges: Measurements and evolution of rubble macroporosity, ridge drilling resistance and consolidated layer strength. *Cold Regions Science and Technology*, V. 151, July 2018, pp. 196-207.
- Grishchenko V.D. (1988). Morphometric characteristics of ice ridges at Arctic basin. Proc. of AARI. V. 401, pp. 46-55 (in Russian with English summary).
- Høyland Knut V. (2007). Consolidation of first-year sea ice ridges. *Journal of Geophysical Research*. 107 (C6, 10.1029/2000JC000526). 15,1-15,15. <https://agupubs.onlinelibrary.wiley.com/doi/10.1029/2000JC000526>
- Høyland K.V. (2007). Morphology and small-scale strength of ridges in the North-western Barents Sea. *Cold Regions Science and Technology*, 48, pp. 169-187.
- Knut V. Høyland & Sveinung Løset. (1999). Experiments and preliminary simulations of the consolidation of a first-year sea ice Ridge. Proc. of the 15th Int. Conf. on Port and Ocean Engineering under Arctic Condition, POAC'99, 1999. Vol. 1, p.49-59.
- ISO19906 (2010). Petroleum and Natural Gas Industries — Arctic Offshore Structures (2010).
- Kharitonov V.V. & Morev V.A. (2011). Method of investigation of internal structure of ice hummocks and stamukhas using the thermal drilling technique. *Russian Meteorology and Hydrology*. V. 36. No. 7: 460-466. <http://mig-journal.ru/archive?id=574>.
- Mironov Y.U., Morev V.A., Porubayev V.S. & Kharitonov V.V. (2003). Study of geometry and internal structure of ice ridges and stamukhas using thermal water drilling. Proc. of the 17th Int. Conf. on Port and Ocean Engineering under Arctic Conditions POAC'03. Trondheim, Norway, June 16-19 2003, V. 2, pp. 623-632.
- Mironov Ye.U. & Porubaev V.S. (2012). Formation of ice ridges in the coastal part of the Kara sea and their morphometric characteristics. *Sovremennye problemy nauki i obrazovaniia. Modern problems of science and education*. No. 4. URL: <http://science-education.ru/ru/article/view?id=6707> (accessed: 05.07.2018).

Mironov Ye.U. & Porubaev V.S. (2005). Structural peculiarities of ice features of the offshore of the Caspian Sea, the Sea of Okhotsk and the Pechora Sea. Proc. of the 18th Int. Conf. on Port and Ocean Eng. under Arctic Conditions (POAC). Potsdam, New York, 26-30 June 2005, Vol. 2, pp. 483-492.

Morev V.A., Morev A.V. & Kharitonov V.V. (2000). Method of determination of ice ridge and stamukha structure, ice features and boundaries of ice and ground. License of Russia № 2153070, Bulletin of inventions № 20 (in Russian).

Pavlov V.A., Kornishin K.A., Efimov Ya.O., Mironov Ye.U. et al. (2016). Peculiarities of consolidated layer growth of the Kara and Laptev Sea ice ridges. Neftyanoe khozyaystvo (Oil industry), No. 11, pp. 49-54 (in Russian with English summary).

Strub-Klein L. & Sodom D. (2012). A comprehensive analysis of the morphology of first-year sea ice ridges. Cold Regions Science and Technology. V. 82, pp. 94–109.

Sodom D. & Timco G. (2013). Knowledge gaps in sea ice ridge properties. Proc. of the 22nd Int. Conf. on Port and Ocean Engineering under Arctic Conditions (POAC). June 9-13, 2013. Espoo, Finland.

Surkov G.A. (2001). Internal structure of first-year hummocks. Proc. of ISOPE, Stavanger, Norway, June 17-22, 2001.

Surkov G.A. (2001). Thickness of the consolidated layer in first-year hummocks. Proc. 16th Int. Conf. on Port and Ocean Engineering under Arctic Conditions. Ottawa, Ontario, Canada. August 12-17, 2001, pp. 245–252.

Tyshko K.P. & Kharitonov V.V. (2011). Some features of one-year ice hummock formation at multiple ice field motions. Russian Meteorology and Hydrology. No. 10, pp. 53-57.

Received on April 3rd, 2019

Accepted on August 8th, 2019